IEEE/CSC SUPERCONDUCTIVITY NEWS FORUM (global edition) January 2015.
This ASC 2014 manuscript 4EPo2E-05 published online in *IEEE Trans. Appl. Supercond.* *(IEEE XPLORE)* DOI: 10.1109/TASC.2014.2363012, on October 15, 2014.

Operation of Mixer Comprising a Series-connected Distributed Superconductor-Insulator-Superconductor Junction Array

Wentao Wu, Jie Liu, Wenlei Shan, *Member, IEEE* and Cheuk-yu Edward Tong, *Member, IEEE*

***Abstract*—Mixers comprising series-connected distributed Superconductor-Insulator-Superconductor tunnel junctions (SDJ) are analyzed. Compared to mixers consisting of parallel-connected distributed junctions (PDJ), SDJ mixers offer wider instantaneous bandwidth and higher dynamic range as well as easier magnetic field tuning. However, SDJ mixers are more complex in operation and in design as well. The reason lies in the fact that the large-signal nonlinear equations containing 3N unknowns, with N the junction number, are difficult to be solved. We propose a fixed-point iterative method to solve the nonlinear equations. This method is verified to be effective and efficient and a case study is done to clarify the uniqueness of SDJ mixers in operation.**

***Index Terms*—Large signal problem, Fixed-point iteration, SIS mixer, Series-connected distributed junctions**

I. Introduction

THE quantum-limited noise performance of Superconductor-Insulator-Superconductor (SIS) mixers makes them ideal for radio astronomical instrumentation. SIS mixer designs have been continuously improved to meet expanding observational requirements, including broader Intermediate Frequency (IF) band and higher dynamic range. The former opens the door for simultaneous observation of multiple molecular lines and at the same time improves the sensitivity of total power or continuum observation, while the latter enables high fidelity mapping by improving the accuracy of amplitude calibration [1]. It has been known that the IF bandwidth and dynamic range are respectively limited by the junction capacitance and the width of the photon step on the pumped IV curve. In order to exceed these limits, SIS mixers comprising series-connected junctions (SJ) are employed, which meet the requirements by reducing the overall capacitance and broadening the photon steps [2]-[4]. In the early years of SIS mixer development, Feldman and Rudner proposed that the analysis of an SJ mixer could be simplified by treating it as a single junction [4]. This approach assumed that all of the junctions of the array are identical and therefore the current is in phase all along the SJ array. We refer it as a series-connected lumped junctions (SLJ). For planar designs, locating all the SIS junctions within a short electrical-distance in the mixer layout approximately justifies the lumped approximation of the array [5], [6]. However, as frequency goes higher or the length of the interconnecting lines between junctions becomes long (intentionally or unintentionally), there would be significant amplitude and phase difference of LO voltage for different junctions in the array. In this case the lumped-element assumption becomes no longer valid and the junction array becomes a distributed one.

If it is properly designed, a series-connected distributed junctions (SDJ), has all the merits a SJ should has [7]-[9]. The most difficult part in SDJ numerical modelling is the algorithm to solve the nonlinear large-signal equation. In the case of an SDJ mixer, standard Newton-Raphson Method is not applicable since the number of unknown variables can be quite large [9], [10]. In order to solve this problem and establish a complete numerical model for SDJ we have developed a fixed-point iteration in this work.

II. Large-Signal Analysis

The purpose of large-signal analysis is to determine the DC bias voltage and LO voltage for each junction by solving the

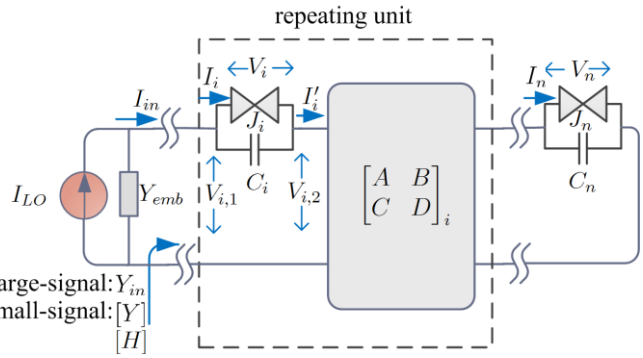

Fig. 1 RF circuit diagram of an SDJ mixer. The SIS junctions are connected through linear networks. Footnote i=1,2,3……N is the sequence number of repeating unit. V_i and I_i stand for LO voltage and current respectively. $I_{i,}$ and $V_{i,2}$ are LO current and voltage at the input port of the ith linear network. $V_{i,1}$ is the LO voltage in front of the ith junction.

This work was partly supported by the National Natural Science Foundation of China under Grants U1331203 and Grants 11073060. This work is also partly supported by Key Laboratory of Radio Astronomy, Chinese Academy of Sciences. *(Corresponding author: Wenlei Shan)*

Wentao Wu is with Purple Mountain Observatory, Chinese Academy of Sciences and Key Laboratory of Radio Astronomy, Nanjing 210008, China. He is also with University of Chinese Academy of Sciences, Beijing, 10040, China(e-mail: wentaowu@pmo.ac.cn)

Jie Liu and Wenlei Shan are with Purple Mountain Observatory, Chinese Academy of Sciences and Key Laboratory of Radio Astronomy, Nanjing, 210008, China (e-mail: jliu@mwlab.pmo.ac.cn, shan@pmo.ac.cn)

Cheuk-yu Edward Tong is with Harvard-Smithsonian Center for Astrophysics, Cambridge, MA 02138 USA (e-mail: etong@cfa.harvard.edu)

IEEE/CSC SUPERCONDUCTIVITY NEWS FORUM (global edition) January 2015.
This ASC 2014 manuscript 4EPo2E-05 published online in *IEEE Trans. Appl. Supercond.* *(IEEE XPLORE)* DOI: 10.1109/TASC.2014.2363012, on October 15, 2014.

LO current balance equation of the SDJ mixer circuit. The generalized schematic of SDJ mixer is plotted in Fig. 1, in which the two adjacent junctions are connected in series through a linear network (usually a section of transmission line) characterized by its ABCD matrix. The large-signal balance equation for the SIS mixers can be written in the following form:

$$f([\alpha_i],[V_{0i}]) = I_{LO}, \tag{1}$$

where the two arrays, $[\alpha_i]$ and $[V_{0i}]$, are LO voltages (normalized by $\hbar\omega_p$, ω_p represents the LO angular frequency) and DC bias voltages of junctions respectively with subscript *i* denoting junctions' sequence number in the array. I_{LO} is the current of LO source. The DC bias voltage and the LO voltage on each junction are related by the following equations reflecting photon-assistant tunneling given by BCS theory:

$$I_{dc,i}(\alpha_i, V_{0i}) = \sum_{n=-\infty}^{n=\infty} J_n^2(\alpha_i) I_{dc,i}(V_{0i} + n\hbar\omega_p / e) \tag{2}$$

$$\begin{aligned} I_i(\alpha_i, V_{0i}) = \sum_{n=-\infty}^{\infty} [&J_n(\alpha_i) J_{n-1}(\alpha_i) I_{R,i}(V_{0i} + n\hbar\omega_p / e) \\ &+ J_n(\alpha_i) J_{n+1}(\alpha_i) I_{R,i}^*(V_{0i} + n\hbar\omega_p / e)] \end{aligned} \tag{3}$$

where, $I_{R,i}(V_{0i})=I_{kk,i}(V_{0i})+iI_{dc,i}(V_{0i})$, $I_{dc,i}(V_{0i})$ is the unpumped DC IV characteristic of the i^{th} junction, $I_{kk,i}(V_{0i})$ is Kramers-Kronig transform of $I_{dc,i}(V_{0i})$, $I_i(\alpha_i,V_{0i})$ is the LO current of the *i*th junction, and J_n is *n*th order Bessel function of the first kind. For an SDJ mixer, the voltages are to be determined. The unknown voltages implicitly depend on LO and DC currents and are presented on the right sides of the Eq. (2) and (3). In consequence the nonlinear Eq. (1) contains 3*N* variables with *N* denoting the number of junctions. In comparison, in PDJ case, the number of unknown variables of Eq. (1) can be reduced to one, since Eq. (2) and (3) are explicit equations. To seek the root for the single unknown, Newton iterative method is effective and efficient. However, if the number of unknowns is large as in the SDJ case, root-seeking by Newton iterative method becomes virtually impossible, which is not only because of the massive calculation in processing the Jacobian matrix but also the difficulty in convergence [10]. For this practical difficulty we resort to an alternative, a fixed-point iterative process, to solve this problem instead.

It is well known that the existence of convergence of a fixed-point iteration strongly depends on the way of construction of the iteration. Our strategy is that the iteration is designed to be an imitation of the physical convergence process of the real system under small perturbation. We believe the natural stability of the system ensures the convergence of the numerical iterative process. The generalized pattern of a fixed-point iteration is

$$[\alpha_i^{k+1}] = g([\alpha_i^k]) \tag{4}$$

where the array $[\alpha_i^k]$ denotes the *k*th iteration result of the normalized LO voltages of the SIS junctions in an SDJ mixer, and g(x) is iterative function. The iterative procedure of solving large-signal problem is summarized as follows and in a flow diagram shown in Fig. 2.

1). As initial values, the LO admittances of the SIS junctions are assumed to be equal to their normal conductance $1/R_n$. Then we are able to calculate the input admittance of the SDJ mixer based on linear network calculation, *i.e.* Y_{in}^k with k=1 shown in Fig. 1.

2). With knowing Y_{in}^k, we calculate the voltage V_{in}^k and the current I_{in}^k at the input port of the network from

$$\begin{cases} V_{in}^k = \dfrac{I_{LO}}{Y_{in}^k + Y_{emb}} \\ I_{in}^k = V_{in}^k Y_{in}^k \end{cases}. \tag{5}$$

3). We then calculate the LO voltage and current on each junction one after another from the first junction to the last one using ABCD matrix

$$\begin{bmatrix} V_{i+1,1}^k \\ I_{i+1}' \end{bmatrix} = \begin{bmatrix} A^k & B^k \\ C^k & D^k \end{bmatrix}_i \begin{bmatrix} V_{i,2}^k \\ I_i' \end{bmatrix}, \tag{6}$$

where $I'_i=I_i+j\omega_p C_i V_i^k$ and C_i is the geometric capacitance of the *i*th junction.

4). Once we know the LO voltage and DC bias current of a junction we can calculate its DC voltage V_{0i}^k by solving Eq. (2). Although this is a nonlinear equation, it has only one unknown variable. Therefore it can be easily solved with standard numerical method.

5). Then we get the updated LO admittance of each junction $Y_i^{k+1} = I_i^k / V_i^k$ with calculated from Eq. (3).

6). Finally we return to step 1) and keep the iteration continuing until a convergence is achieved.

This algorithm generally can come to a convergence within several times iteration. After the bias voltage and LO voltage for each junction are solved, the small-signal analysis and noise analysis can be conducted to evaluate the mixer performances.

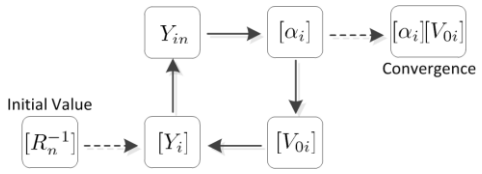

Fig. 2 Flow chart of the fixed-point iteration for the numeric solution of large-signal equations for an SDJ mixer.

III. Small Signal And Noise Analysis

Small-signal and noise analysis are linear analysis based on matrix calculation. The conversion admittance matrix (Y matrix) and noise current correlation matrix (H matrix) for each embedded junction are readily calculated using Tucker's quantum mixing theory [11] once the LO voltage and DC bias

IEEE/CSC SUPERCONDUCTIVITY NEWS FORUM (global edition) January 2015.
This ASC 2014 manuscript 4EPo2E-05 published online in *IEEE Trans. Appl. Supercond.* *(IEEE XPLORE)* DOI: 10.1109/TASC.2014.2363012, on October 15, 2014.

TABLE I
Y AND H MATRIX REDUCTION PROCESS

Operation	[Y]	[H]
(a)	$[\mathbf{Y}] = [\mathbf{Y}_1] + [\mathbf{Y}_2]$	$[\mathbf{H}] = [\mathbf{H}_1] + [\mathbf{H}_2]$
(b)	$[\mathbf{Y}] = ([\mathbf{Y}_1]^{-1} + [\mathbf{Y}_2]^{-1})^{-1}$ With: $[\mathbf{E}] = ([\mathbf{Y}_1] + [\mathbf{Y}_2])^{-1}[\mathbf{Y}_2]$, $[\mathbf{F}] = ([\mathbf{Y}_1] + [\mathbf{Y}_2])^{-1}[\mathbf{Y}_1]$	$[\mathbf{H}] = [\mathbf{E}][\mathbf{H}_1][\mathbf{E}]^\dagger + [\mathbf{F}][\mathbf{H}_2][\mathbf{F}]^\dagger$
(c)	$[\mathbf{Y}] = ([\mathbf{C}] + [\mathbf{D}][\mathbf{Y}_1]) \cdot ([\mathbf{A}] + [\mathbf{B}][\mathbf{Y}_1])^{-1}$ With: $[\mathbf{T}] = [\mathbf{D}] - [\mathbf{Y}][\mathbf{B}]$	$[\mathbf{H}] = [\mathbf{T}][\mathbf{H}_1][\mathbf{T}]^\dagger$

(a) connection of two noisy one-ports in parallel, (b) connection of two noisy one-ports in series, and (c) combination of a noiseless two-port and a load. Note that it is assumed that all noise sources are independent.

voltage are determined from the large-signal analysis. The overall effective Y matrix and the H matrix for the whole array are derived using a set of array-reduction operations. Based on Norton's theorem, each operation reduces the array by replacing the two elements at the far end of the array with a single effective load and a noise current source. The effective load does not affect the response to the input signal and the effective noise current source generates the same noise power on the IF load as the unreduced network does. The operation is repeated until the final effective Y matrix and H matrix are achieved.

There are three kinds of operations in the process of the array reduction: (a) connection of two noisy one-ports in parallel, (b) connection of two noisy one-ports in series, and (c) combination of a noiseless two-port and a noisy load. The effective Y and H matrices of these operations are listed in Table I with the assumption that all noise sources are independent. We apply N-frequency matrices (N is the number of frequencies involved in the small signal analysis) in formulating the effective Y and H matrices following [7].

IV. Simulation Results

A. *Verification of the fixed-point iteration*

In order to evaluate the feasibility of this fixed-point iterative method, we compare the two methods (Newton and this one) by means of simulating the PCTJ mixer designed for ALMA band 8 [12]. In this design, the critical current density is 10kA/cm^2, and the junctions are measuring 1μm in diameter. The normal-state resistance of each SIS junction based on Nb film is about 26 Ω and the junction's specific capacitance is estimated to be 90 fF/μm^2. The simulation results are shown in Fig. 3. The simulated gain and noise are identical with each other. It is found that the efficiency of convergence of this fixed-point iteration is comparable or even better than the Newton method with the almost same time per pass. This is evident in the inset of Fig. 3, in which an example of convergence chart is plotted.

B. *SDJ mixer simulation results*

The fixed-point iterative method investigated in this paper

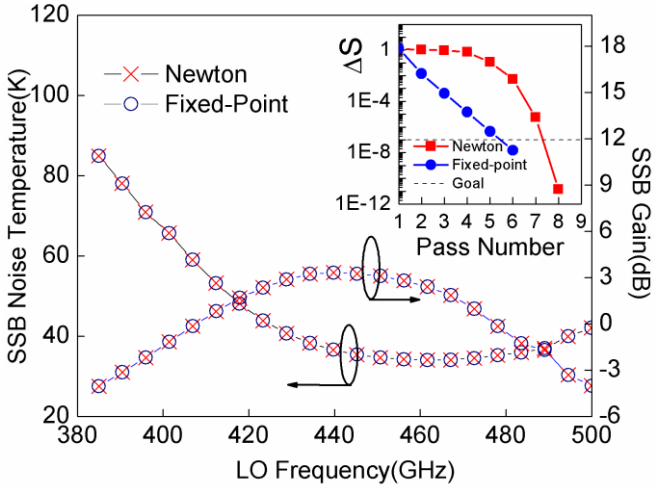

Fig. 3 Comparison in accuracy and efficiency of two iterative methods (Newton and fixed-point) in simulating a 450 GHz band SIS mixer. The inset shows an example of convergence diagram for efficiency comparison.

is aimed to solve the large-signal problem for an SDJ mixer. It allows us to simulate the mixer performances that previously difficult to do. Two most significant capabilities gained from this new method are simulation of the pumped IV curves and optimization the operation state including bias current and LO power. As a case study, we carried out simulations of a 220 GHz band SDJ mixer of N=3 reported in [13] to demonstrate the significance of this simulation technology and investigate the uniqueness of SDJ mixer in optimizing the LO power and bias current. For this SDJ mixer, the target critical current density is ~ 7kA/cm^2, and the junctions are nominally 1.7 μm in diameter. This gives a normal state resistance of about 12 Ω per junction, with a specific junction capacitance of 85 fF/μm^2. As for superconducting microstrip circuit based on a 250 nm-thick SiO_2 thin film, the wiring layer is 600 nm thick and the base layer is 150 nm thick Nb. A quarter-wave transformer section is employed to further match to the source impedance (~ 40Ω).

The SIS junctions embedded in the SDJ are pumped

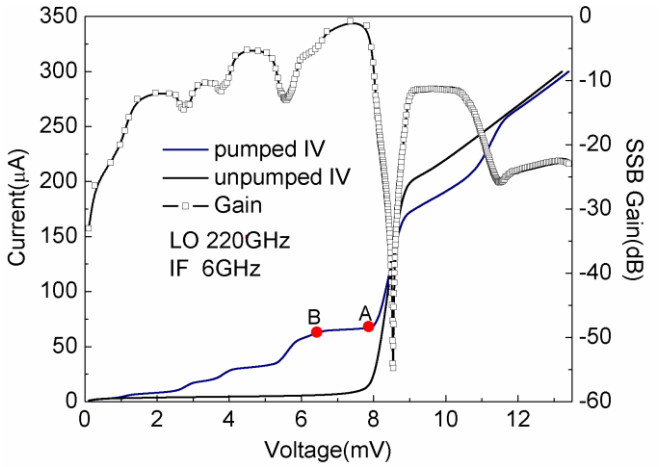

Fig. 4 Simulated IV characteristics and conversion gain of the 3-junction SDJ mixer with optimal LO pumping at 220 GHz. The conversion gain is calculated at an IF of 6 GHz. The bias ranging between A and B is the tuning range to optimize for the highest gain.

IEEE/CSC SUPERCONDUCTIVITY NEWS FORUM (global edition) January 2015.
This ASC 2014 manuscript 4EPo2E-05 published online in *IEEE Trans. Appl. Supercond.* *(IEEE XPLORE)* DOI: 10.1109/TASC.2014.2363012, on October 15, 2014.

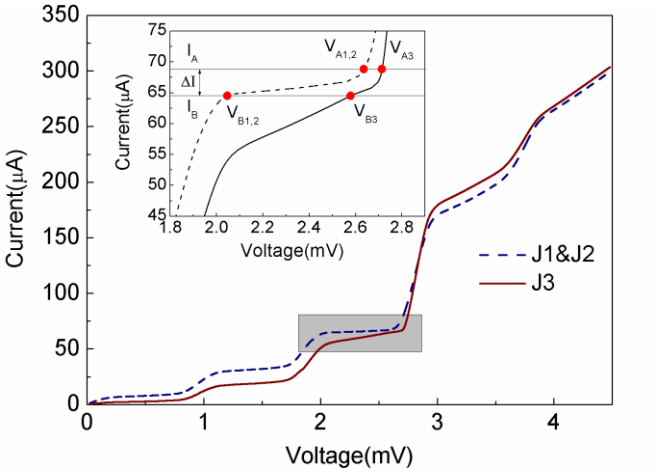

Fig. 5 Breakdown IV curves for individual junctions of the IV curve in Fig. 4. The inset enlarges the tuning range ΔI so that we can clearly see the bias voltage of each junction. The $V_{A1,2}$ and V_{A3} represent the bias voltage of junction 1(2) and 3 respectively when the bias current is I_A , and the $V_{B1,2}$ and V_{B3} are those when the current is I_B.

unequally since they are distributed along the LO path. Because of the difference in photon step height but the same current in DC bias in each junction, their bias voltages result to be different. This makes tuning of the SDJ mixers more complicated than PDJ mixers. The complexity in operation SDJ can be observed from the overall pumped IV curve and the breakdowns for each element as shown in Fig. 4 and Fig. 5 respectively. In Fig. 4 we plot the simulated pumped IV curve of the overall array together with its conversion gain. The pump power is optimized to achieve the highest gain. Two bias current values (A and B) presented in Fig. 4 mark the -3dB-gain tuning range, which covers almost the full width of the photon step in voltage. In Fig. 5, the pumped IV curves of individual junctions are plotted. Because they are the same in size and close in location, J1 and J2 are pumped to the same level. In comparison, J3 is not pumped as high as J1 and J2. In addition to the difference in pumping level, the slopes of photon steps of these junctions are different. It is because that the source impedance as respect to a specific junction includes all other junctions being unequally pumped and biased in voltage. Therefore the source impedances are different from each other.

When the device is bias at point A, J1 and J2 are biased at the rear part of the photo step where they can still provide reasonable conversion efficiencies, but J3 is idling since it is biased at the gap voltage and the dynamic resistance is measured to be 0.5 Ω. In the other extreme, when the mixer is based at point B, J1 and J2 are biased at the rising edge of the photon step and J3 is biased away from but still close to the gap voltage where the dynamic resistance is about 50 Ω. In this operation condition all of the junctions are marginally biased to be functional for mixing. In between of the two extremes, an optimal bias exists to give the highest conversion efficiency. At this optimal bias, J1 and J2 are properly biased for mixing while J3 provides RF grounding and does not contribute much to mixing. This is the operation mode adopted in [9] and [13].

It's worth noting that in some cases we encountered failures in convergence if the dynamic resistance at the bias voltage is negative. In fact when the mixer is biased on negative slope Newton iteration is also difficult to reach convergence. Since at practical applications it may cause instability in the bias supply, negative dynamic resistance is intentionally excluded in the design phase.

V. Conclusion

We have developed a fixed-point iterative method to solve the large-signal nonlinear equations of SIS mixers, which is especially useful for SDJ mixers simulation since Newton iterative method can be hardly applied due to too many un-known variables. This method has been verified to be efficient in convergence in solving SDJ problem by revisiting a 3-junction SDJ design. This method substantially enhances the simulation capability in design and analysis of SDJ mixers.

Compared to SLJ mixers, in which the junctions should act as a single lumped element, SDJ circuitry gains more freedom in design of high performance devices with broad IF band, RF band as well as dynamic range. We believe this work is beneficial to these developments and bring about new ideas in the mixer design to further expend the IF bandwidth of SIS mixers.

References

[1] M.J.Feldman and L.R.D' Addario, "Saturation of the SIS Direct Detector and the SIS Mixer," *IEEE Trans. Magnetics*, vol.MAG-23, in press, 1987.

[2] S. Rudner and T. Claeson, "Arrays of Superconducting Tunnel Junctions as Low Noise 10-GHz Mixers," *Appl. Phys. Lett.*, vol. 34, no. 10, pp. 711-713, 15 May 1979.

[3] Kerr, A.R., S.-K. Pan, M.J. Feldman and A. Davidson, "Infinite available gain in a 115 GHz SIS mixer," *Physica B+C*, vol. 108, pp. 1369–1370, August 1981.

[4] M.J. Fe1dman and S. Rudner," MIXING WITH SIS ARRAYS", *Reviews of Infrared and Millimeter Waves*, vol. 1, pp. 47-75, 1983.

[5] A. R. Kerr, S.-K. Pan, A. W. Lichtenberger and H. H. Huang, "A tunerless SIS mixer for 200–280 GHz with low output capacitance and inductance", *in Proc. 9th Int. Symp. Space THz Tech.*, pp. 195-203, March 1998,

[6] Anthony R. Kerr, Shing-Kuo Pan, St ́ephane M. X. Claude *et al*, "Development of the ALMA-North America Sideband-Separating SIS Mixers" *IEEE MTT-S International Microwave Symposium Digest (IMS)*, pp. 1-4, June 2013.

[7] C.-Y. E. Tong and R. Blundell, "Theory of series-connected distributed SIS mixers with ultra-wide instantaneous bandwidth," *in Proc. 17th Int. Symp. Space THz Tech.*, pp.35-38, May 2006.

[8] C.-Y.E. Tong et al, "A distributed lumped-element SIS mixer with very wide instantaneous bandwidth," *IEEE Trans. Appl. Supercond.*, vol. 15, no. 2, pp. 490-494, June 2005.

[9] Cheuk-yu Edward Tong et al," Design and Performance of a 3-Junction Series Distributed SIS Mixer for Wide IF Applications", *IEEE Trans. Appl. Supercond.*, vol. 23, no. 3, June 2013

[10] William H. Press, Saul A. Teukolsky, William T. Vetterling *et al.*, *Numerical Recipes in C: The Art of Scientific Computing* 2nd ed., vol. 9. Cambridge University Press, 1992, pp. 379–383.

[11] J.R.Tucker, and M.J. Feldman, "Quantum detection at millimeter wavelengths", *Rev. Mod. Phys.*, vol. 57, pp. 1055-1113, 1985.

[12] Wenlei Shan, Takashi Noguchi, Shengcai Shi, et al, "Design and Development of SIS Mixers for ALMA Band 8", *IEEE Trans. Appl. Supercond.*, vol. 15, no. 5, June 2005.

[13] Cheuk-Yu Edward Tong, Paul Grimes, Raymond Blundell, Ming-Jye Wang, and Takashi Noguchi," Wideband SIS Receivers Using Series Distributed SIS Junction Array", *IEEE Trans on Terahertz Science and Technology*, vol. 3, no. 4, July 2013.